5th ECPMG Delft · 2024

Proceedings of the 5th ECPMG 2024
5th European Conference on Physical Modelling in Geotechnics
2-4 October 2024, Delft, the Netherlands

Centrifuge model for uplift and heave in clay layers

L.V. Cote
Delft University of Technology, Delft, The Netherlands, L.CoteMartinez@tudelft.nl

B. Wittekoek
Deltares, Delft, The Netherlands, Britt.Wittekoek@deltares.nl

C. Zwanenburg
Delft University of Technology, Delft, The Netherlands, Cor.Zwanenburg@deltares.nl

Deltares, Delft, The Netherlands, C.Zwanenburg@tudelft.nl

M.A. Cabrera
Delft University of Technology, Delft, The Netherlands, M.A.Cabrera@tudelft.nl

ABSTRACT: Flood protection structures, like dikes or levees, are crucial for coastal and deltaic regions around the world. These structures often stand over a low-permeable foundation layer that spans from the water body up to tens of meters into the protected land, sustaining the structure's weight and preventing seepage flow to emerge. Uplift and heave are among the failure mechanisms that could compromise the effectiveness of the flood protection structure. In this work, the goal is to describe the driving mechanisms for uplift and heave to develop in a clay layer, when subjected to upward flow in a centrifuge model. We vary the clay layer thickness, while exploring the layer response under different acceleration levels by means of pore-pressure measurements and digital image analysis. We identify the transition from the layer bending to the appearance of surface cracks that facilitate seepage flow. The observations gained from these experiments help in shedding light on the limiting conditions for foundation layers under extreme loading and link them with the structure's stability.

1 INTRODUCTION

Flood protection structures, like dikes or levees, consist of an earthen structure that separates a water course (*e.g.,* river, canal) or water body (*e.g.,* lake, sea, reservoir) from a floodplain area. Due to its simplicity and easiness of construction, dike structures are common in coastal and deltaic regions around the world. On some occasions, a dike may lay over a low-permeable layer that covers a permeable layer, extending up to a couple of tens of meters over the floodplain side (*i.e.,* hinterland), accompanied by a ditch that reduces its effective thickness. Under such a stratified configuration, the low-permeable layer might deform due to fluid pressures coming from the permeable layer or by the action of the dike's self-weight (Cooling & Marsland, 1953). The vertical deformation of the low-permeable layer can be accentuated by increments in the level and frequency at which the water loading oscillates. Under severe conditions, the dike stability could be compromised, by a reduced lateral bearing capacity or the progression of internal erosion processes associated to the formation of cracks (Van *et al.,* 2005).

Uplift is understood to appear when the pore pressures on the permeable layer rise as high as the weight of the overlaying layer. At that point, a thin layer of water is assumed to form between the soil layers, eliminating any shear resistance at its interface (Van *et al.,* 2005). As a result, the groundwater flow through the permeable layer adapts to an upward pressure, extending horizontally up to an equilibrium length. Under this new loading configuration, the low-permeable layer heaves, buckling and potentially cracking when the bending capacity is exceeded. Interestingly, clay layers in the field are rarely reported to exhibit cracks by groundwater flow and their bending are then incorporated into a compound interaction mechanism with the dike structure (Hird *et al*., 1978; Padfield & Schofield, 1983*;* Allersma & Rohe, 2003; Van *et al.*, 2005). Nevertheless, it remains unclear whether the layer cracking is not being recognised as part of a dike failure, either because of the complexity of the resultant failure mechanism or because of unawareness.

In this work, we aim to describe the driving mechanisms for uplift and heave to develop in a clay layer, when subjected to upward flow in a centrifuge model. We vary the clay layer thickness, while exploring the layer response under different acceleration levels by means of pore-pressure

measurements and digital image analysis. The insight gained from these experiments would contribute to the understanding of the coupled interaction of dike and low-permeable layers (Cengiz *et al.*, 2024).

2 METHODOLOGY

The stratified system is simplified by a single clay layer laying over a porous platform. This system is meant to be analogous to the ditch in a low-permeable layer. The porous platform connects to a reservoir, where the fluid head pressure H can be increased by activating a valve that connects with a top tank (see Fig. 1). The model assumes that drainage occurs only perpendicular to the clay layer from bottom to top. Additionally, side stopers are placed at the clay layer ends promoting its bending at the centre. By this configuration, we aim at reproducing the layer bending under plane-strain conditions.

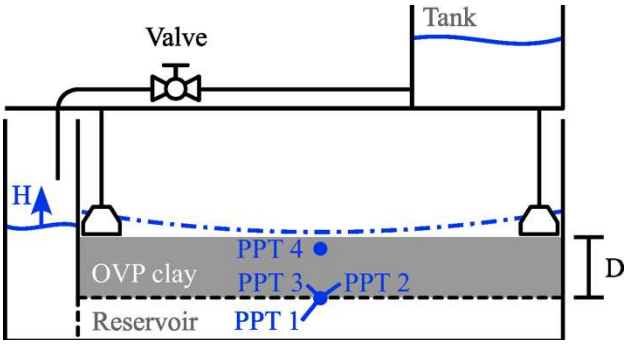

Figure 1. Schematic of the experimental model of an OVP clay layer of thickness D. The dashed lines mark permeable elements inside the model and the dash-dotted line illustrates the water free-surface curvature induced by the centrifugal acceleration field.

The clay layer consists of Oostvaardersplassen (OVP) clay, consolidated outside the centrifuge up to a pressure of 20 kPa. The OVP clay layer preparation follows the same procedure as described in Fern *et al.* (2017). OVP clay has a saturated unit weight of 13.4 kN/m^3 and permeability of 4.9×10^{-5} m/day. In this work, we focus on two clay layer thicknesses D = [40; 60] mm, and keep the layer length of 460 mm and width of 150 mm constant. The fluid used in experiments is tap water, and the top tank is filled with 2.5 l.

The experiments are conducted at TU Delft 1.3 m radius beam centrifuge (Allersma, 1994). The model container is an aluminium strongbox of 555 mm long, 220 mm high, and 180 mm wide, covered on top by an aluminium plate carrying a 4.5 l water tank. The water tank is connected to the model reservoir by a 12 mm aluminium pipe, activated by a solenoid valve. The model is placed in the rotational plane, perpendicular to the centrifuge axis of rotation, inducing a curvature on the water free surface (see dash-dotted line in Fig. 1). As a result, the OVP clay layer is covered by an additional 10 mm of water before testing, with the objective of preventing drying during spin-up.

The evolution of fluid pressures during testing are monitored with four pore pressure transducers (PPT) with a porous ceramic with air entry of 1 bar and aligned at the centre of the clay layer. PPT 1 and PPT 2 are located at the porous platform, measuring the fluid pressures at the reservoir, with PPT1 being oriented horizontally, and PPT2 pointing upwards at the porous platform and in contact with the clay. PPT 3 is placed on the model back wall, at the level of the porous platform, and PPT 4 is placed 20 mm above the porous platform and in contact with the OVP clay layer. Additionally, the OVP clay layer deformation is recorded through a 15 mm thick side polymethyl methacrylate (PMMA) window at a frame rate of 25 fps and with a resolution of 1280 by 720 px, equivalent to approximately 0.5 mm/px.

The experimental protocol initiates by placing the OVP clay layer inside the strongbox and filling in the reservoir, surface layer, and top tank. The model is then spun up to an equivalent acceleration of 50*g* and left for 30 minutes. Then, the solenoid valve is activated and the PPT measurements are recorded at a sampling rate of 10 Hz. Due to a connection issue, the test with D = 60 mm was consolidated at 50*g*, but the solenoid valve had to be activated at 30*g*.

3 RESULTS AND DISCUSSION

Prior to the valve activation, the water free surface above the clay layer and inside the reservoir curves aligns with the centrifugal acceleration field. However, their curvatures do not match, indicating that seepage has not occurred through the OVP clay layer yet. After the valve opens, the reservoir rapidly fills in, and the OVP clay layer starts to deform before all water evacuates the tank (see Fig. 2). For tests with D = 40 mm (at 50*g*) and D = 60 mm (at 30*g*) the onset of deformation happens at H = 35 mm and H = 60 mm in model scale, respectively. Then, the clay layer deforms until reaching a maximum height, while the reservoir continues filling in until the top tank is almost empty. Interestingly, the layer with D =40 mm develops a series of cracks at its peak deformation, allowing water to pass by the layer (see Fig. 2(a-b)). After this instant, the water height above the layer and in the reservoir balances and the cracks seal, leaving the clay layer back to its initial configuration. On the contrary, the layer with D = 60 mm reaches its

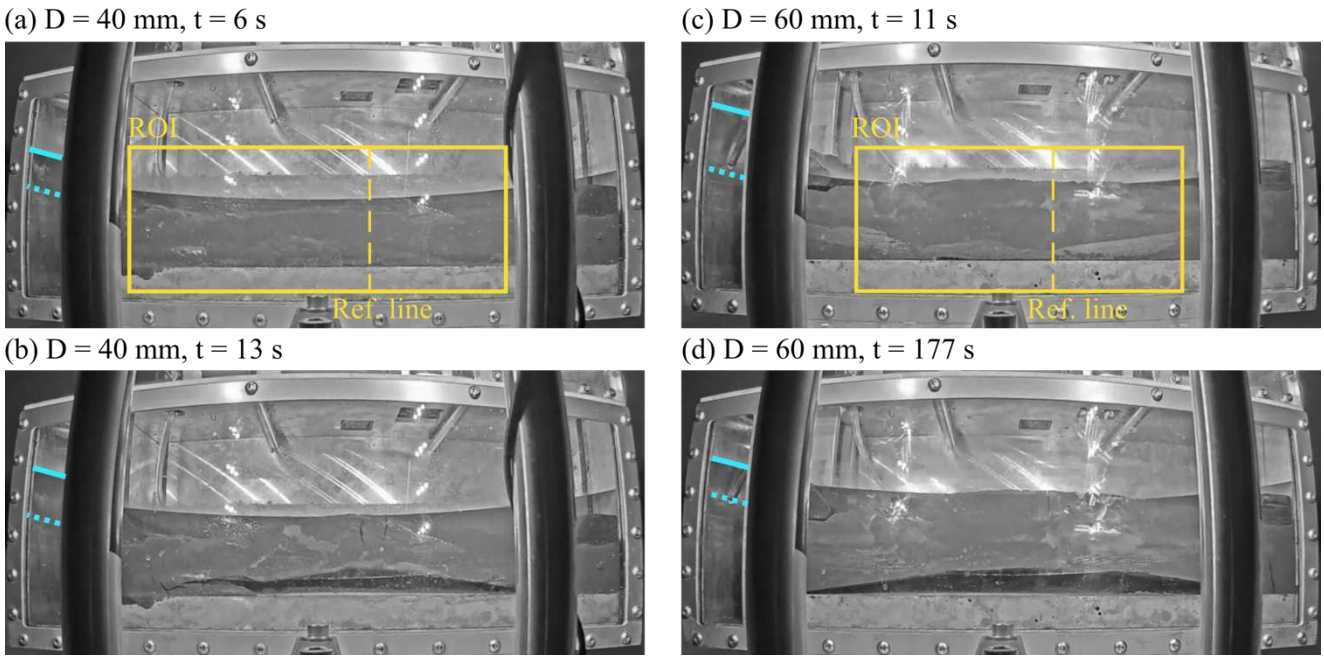

Figure 2. Snapshots for test with a OVP clay layer thickness of (a-b) D = 40 mm and (c-d) D = 60 mm. The instants (a) and (c) mark the onset of deformation and instants (b) and (d) mark the maximum observed deformation. The frame inside the top images represents the region of interest (ROI) for the space-time analysis, and the blue dashed and continuous lines on the right of each snapshot show the initial and instantaneous water level, respectively.

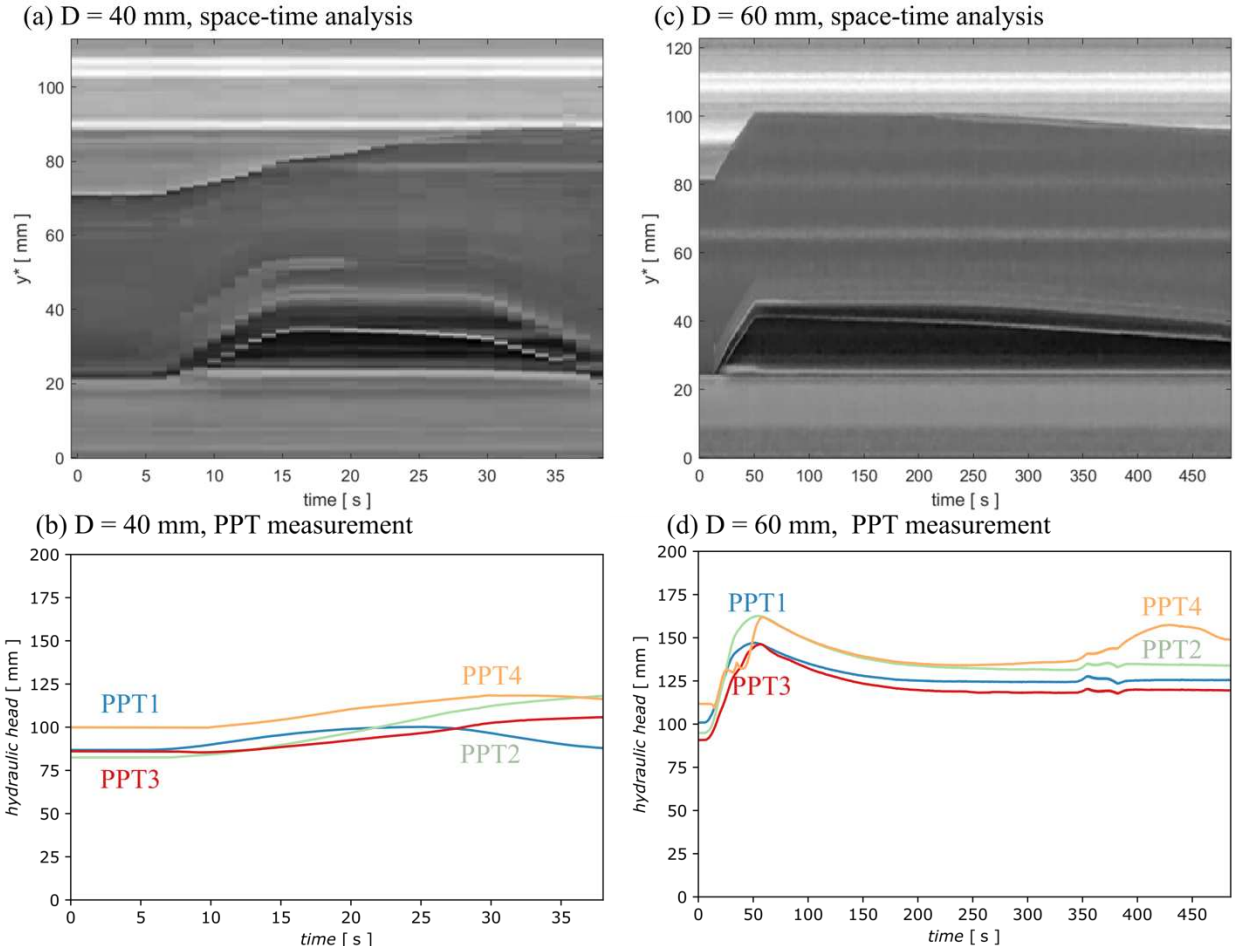

Figure 3. Results from tests (a-b) D = 40 mm and (c-d) D = 60 mm. The top row presents the space-time analysis (a,c) and the bottom row the equivalent hydraulic head from pore pressure measurements (b,d).

maximum deformation with some partial cracks on the surface (see Fig. 2(c-d)) and remains suspended until the acceleration level is varied.

The rapid uplift and occasional collapse or suspension of the OVP clay layer can be analysed by means of a space-time analysis within a common region of interest (ROI) in all frames (Cabrera & Wu, 2017). The reference line for the space-time analysis is selected at the horizontal location of the apex of deformation (see dashed line in Fig. 2(b-d)). From this analysis, the rate at which the layer rises is 1.2 mm/s and 0.8 mm/s for tests D = 40 mm and D = 60 mm, respectively (see Fig. 3(a,c)). Moreover, the elapsed time until the layer returns to its initial configuration is 19 s for test D = 40 mm, while in a similar period only a marginal change in the layer thickness is observed for D = 60 mm (see Fig. 3(a,c)).

The PPT measurements provide a closer look at the consolidation process before activating the valve (PPT4), not shown in Fig. 3, then the subsequent build-up of pore pressures beneath the OVP clay layer after valve activation (PPT1 to PPT3), and its dissipation during layer deformation (PPT1 to PPT3). At first sight, it is remarkable that uplift in test D = 40 mm last for about 25 s (see Fig. 3(b)), building up pressures at the clay layer and beneath, while starting to decrease at the reservoir (PPT1). Note that only PPT1 resembles the deformation pattern shown on Fig. 3(a), indicating that some residual fluid pressures remain after the layer collapses on other PPTs. On the contrary, test D = 60 mm shows a collective pressure build up at all locations (see Fig. 3(d)), reaching a maximum at peak upfit (see Fig. 3(c)) and dissipating at about a common rate after the peak. The build-up of pressures at the clay layer (PPT4 in Fig. 3(d)) might indicate a coupled mechanism with the layer deformation, as no hydraulic connectivity is expected between the layer and reservoir. Further work focuses on the interpretation of pore pressures beneath the clay layer, aiming at clarifying the small disparity, of about 5 mm of equivalent hydraulic head, between PPT1 to PPT3.

4 CONCLUSIONS

This paper presents the experimental results from a novel uplift test on a OVP clay layer. The tests successfully visualize the layer deformation and associated formation of cracks by means of digital image analysis and pore pressure measurements. For the test with a thickness of D = 40 mm, a series of cracks expand over the whole layer, allowing the dissipation of the basal fluid pressures followed by the crack sealing and layer reconfiguration. For the test with a thickness of D = 60 mm, a visible crack form on the layer surface, but it does not cross fully, leaving the layer suspended until the acceleration level is changed.

These series of experiments provide a unique insight into the mechanisms behind uplift and heave in clay layers, indicating that uplift does lead to the formation of cracks, but that these will seal if the layer is fully transversed by them. Ongoing testing will explore the governing effects of layer thickness and fluid viscosity, aiming at evaluating the need of accounting for crack formation in the macro-stability analysis for dikes. The relevance of this series of experiments helps in pointing out that cracks due to uplift can be expected at the ditch, and hence be reflected in the stability analysis of the flood protection structure.

ACKNOWLEDGEMENTS

The authors would like to thank R. Klasen for his assistance in the preparation and execution of experiments. This work received financial support by the National Flood Protection Programme (HWBP) and the water authority Drents Overijsselse Delta, WDOD.

REFERENCES

Allersma, H. G. B. (1994). The University of Delft geotechnical centrifuge. In *International conference centrifuge 94* (pp. 47-52).

Allersma, H. G. B., and Rohe, A. (2003). Centrifuge tests on the failure of dikes caused by uplift pressure. *International Journal of Physical Modelling in Geotechnics, 3*(1), 45-53. https://doi.org/10.1680/ijpmg.2003.030104

Cabrera, M. A., and Wu, W. (2017). Space–time digital image analysis for granular flows. *International Journal of Physical Modelling in Geotechnics, 17*(2), 135-143. https://doi.org/10.1680/jphmg.16.00018

Cengiz, C., Cabrera, M. A., Wittekoek, B., Fransen, M., Wopereis, L., and Zwanenburg, C. (2024). Centrifuge tests on the uplift and deformation patterns of clay cover layers in deltas. In *Proceedings of the XVIII ECSMGE*, Lisbon.

Cooling, L. F., and Marsland, A. (2011). Soil mechanics studies of failures in the sea defence banks of Essex and Kent. In *Conference on the North Sea floods of 31 January/1 February, 1953* (pp. 58-73). Thomas Telford Publishing.

Hird, C. C., Marsland, A., and Schofield, A. N. (1978). The development of centrifugal

models to study the influence of uplift pressures on the stability of a flood bank. *Géotechnique, 28*(1), 85-106. https://doi.org/10.1680/geot.1978.28.1.85

Fern, E. J., de Lange, D. A., Zwanenburg, C., Teunissen, J. A. M., Rohe, A., and Soga, K. (2017). Experimental and numerical investigations of dyke failures involving soft materials. *Engineering Geology, 219,* 130-139. https://doi.org/10.1016/j.enggeo.2016.07.006

Padfield, C. J., and Schofield, A. N. (1983). The development of centrifugal models to study the influence of uplift pressures on the stability of a flood bank. *Géotechnique, 33*(1), 57-66. https://doi.org/10.1680/geot.1983.33.1.57

Van, M. A., Koelewijn, A. R., and Barends, F. B. J. (2005). Uplift phenomenon: Model, validation, and design. *International Journal of Geomechanics*, 5(2), 98-106. https://doi.org/10.1061/(ASCE)1532-3641(2005)5:2(98)